Nuku'alofa

Chapter 14
Tonga

The contributions of Ofa Fa'anunu and Mele Lakai from the Tonga Meteorological Service are gratefully acknowledged

Introduction

This chapter provides a brief description of Tonga, its past and present climate as well as projections for the future. The climate observation network and the availability of atmospheric and oceanic data records are outlined. The annual mean climate, seasonal cycles and the influences of large-scale climate features such as the South Pacific Convergence Zone and patterns of climate variability (e.g. the El Niño-Southern Oscillation) are analysed and discussed. Observed trends and analysis of air temperature, rainfall, extreme events (including tropical cyclones), sea-surface temperature, ocean acidification, mean and extreme sea levels are presented. Projections for air and sea-surface temperature, rainfall, sea level, ocean acidification and extreme events for the 21st century are provided. These projections are presented along with confidence levels based on expert judgement by Pacific Climate Change Science Program (PCCSP) scientists. The chapter concludes with a summary table of projections (Table 14.4). Important background information including an explanation of methods and models is provided in Chapter 1. For definitions of other terms refer to the Glossary.

14.1 Climate Summary

14.1.1 Current Climate

- Sites in Tonga show some seasonal variations in air temperature due to their position close to the sub-tropics. Part of the seasonal change is driven by the sea-surface temperature of the oceans surrounding the islands.
- Nearly two-thirds of Tonga's rainfall falls in the wet season from November to April. The rainfall is affected by the South Pacific Convergence Zone, which is most intense during the wet season.
- Rainfall in Tonga has high variability from year-to-year due mainly to the El Niño-Southern Oscillation.
- Warming trends are evident in both annual and seasonal mean air temperatures at Nuku'alofa for the period 1950–2009, with the strongest trends in the wet season.
- Annual and seasonal rainfall trends for Nuku'alofa and Lupepau'u for the period 1950–2009 are not statistically significant.
- The sea-level rise near Tonga measured by satellite altimeters since 1993 is over 6 mm per year.
- On average, Nuku'alofa experiences 17 tropical cyclones per decade, with most occurring between November and April. The high interannual variability in the tropical cyclone numbers makes it difficult to identify any long-term trends in frequency.

14.1.2 Future Climate

Over the course of the 21st century:

- Surface air temperature and sea-surface temperature are projected to continue to increase (*very high* confidence).
- Wet season rainfall is projected to increase (*moderate* confidence).
- Dry season rainfall is projected to decrease (*moderate* confidence).
- Little change is projected in annual mean rainfall (*low* confidence).
- The intensity and frequency of days of extreme heat are projected to increase (*very high* confidence).
- The intensity and frequency of days of extreme rainfall are projected to increase (*high* confidence).
- Little change is projected in the incidence of drought (*low* confidence).
- Tropical cyclone numbers are projected to decline in the south-east Pacific Ocean basin (0–40ºS, 170ºE–130ºW) (*moderate* confidence).
- Ocean acidification is projected to continue (*very high* confidence).
- Mean sea-level rise is projected to continue (*very high* confidence).

14.2 Country Description

Tonga is located in the western South Pacific Ocean, between 15°–23.5°S and 173°–177°W. The archipelago is spread over 800 km in a north-south direction. Tonga consists of four groups of islands: Tongatapu and 'Eua in the south, Ha'apai in the middle, Vava'u in the north and Niuafo'ou and Niua Toputapu in the far north. The 172 named islands have an area of 748 km^2. The islands include high volcanic islands, elevated limestone islands and low-lying atolls. The area of the Exclusive Economic Zone is 720 000 km^2. The capital, Nuku'alofa, is situated in Tongatapu in the south (Tonga's Joint National Action Plan, 2010). The 2010 estimated population was 103 365 (Tonga Country Statistics, SOPAC, 2010).

Agricultural production is the main economic sector with squash, coconuts, bananas, and vanilla beans comprising the main crops. Agricultural exports make up two-thirds of total exports. The tourism sector is growing in importance (Tonga's Pacific Adaptation to Climate Change, 2006).

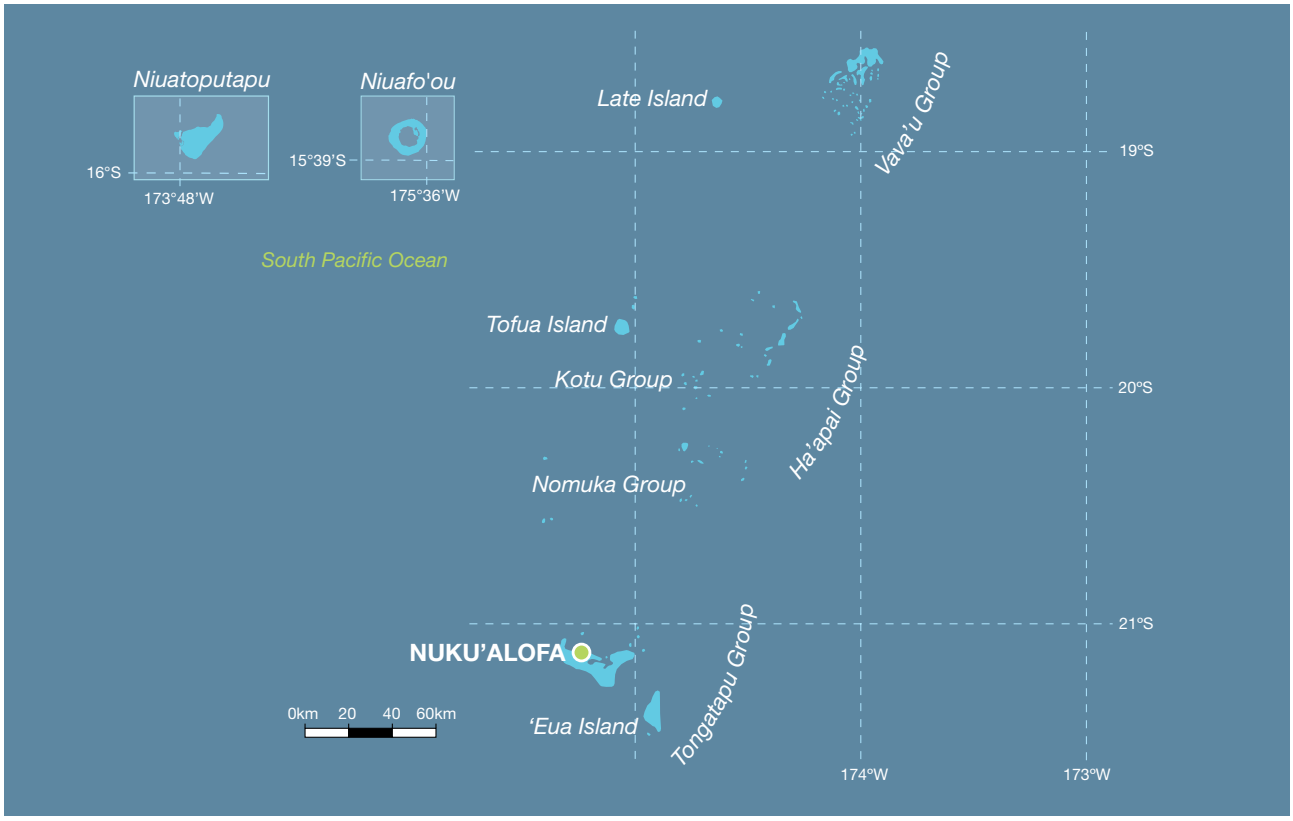

Figure 14.1: Kingdom of Tonga

14.3 Data Availability

There are currently seven operational meteorological stations in Tonga. Multiple observations within a 24-hour period are taken at Fua'amotu, Lupepau'u (also known as Vava'u), Niuatoputapu (also known as Keppel), Ha'apai and Niuafo'ou. A single daily observation is taken at Nuku'alofa and Kaufana. Nuku'alofa and Fua'amotu, the primary stations, are located on the northern and southern side of Tongatapu Island respectively. Nuku'alofa has rainfall data from 1944 and air temperature data from 1945 and Lupepau'u, Ha'apai and Niuatoputapu have rainfall data from 1947 and temperature data from 1950. Additional data for the period 1931–1941 have recently been discovered in the United Kingdom. These data are yet to be digitised.

Nuku'alofa and Lupepau'u rainfall and air temperature records from 1950 (Lupepau'u temperature from 1956) have been used. Both records are homogeneous and more than 95% complete.

Oceanographic records do not cover such a long time period. Monthly-averaged sea-level data are available from 1993 at Nuku'alofa (1993–present). A global positioning system instrument to estimate vertical land motion was deployed at Nuku'alofa in 2002 and will provide valuable direct estimates of local vertical land motion in future years. Both satellite (from 1993) and in situ sea-level data (1950–2009; termed reconstructed sea level; Volume 1, Section 2.2.2.2) are available on a global 1° x 1° grid.

Long-term locally-monitored sea-surface temperature data are unavailable for Tonga, so large-scale gridded sea-surface temperature datasets have been used (HadISST, HadSST2, ERSST and Kaplan Extended SST V2; Volume 1, Table 2.3).

14.4 Seasonal Cycles

Sites in Tonga show some seasonal variations in air temperature due to their position close to the sub-tropics. Being further south, Nuku'alofa has a slightly larger difference in air temperatures (about 5ºC) between the warmest month (February) and the coolest (July-August) months than Lupepau'u. Part of the seasonal change is driven by temperatures of the oceans surrounding the islands of Tonga. Air temperatures in the winter months are also affected by sub-tropical high pressure systems that direct cooler air from the south.

Both Nuku'alofa and Lupepau'u have marked seasonal cycles in rainfall, particularly Lupepau'u. Almost two-thirds of the annual rainfall comes during the wet season from November to April. The remainder falls in the dry season from May to October. This reflects the importance of the South Pacific Convergence Zone (SPCZ) on rainfall in Tonga, which is most intense during the wet season.

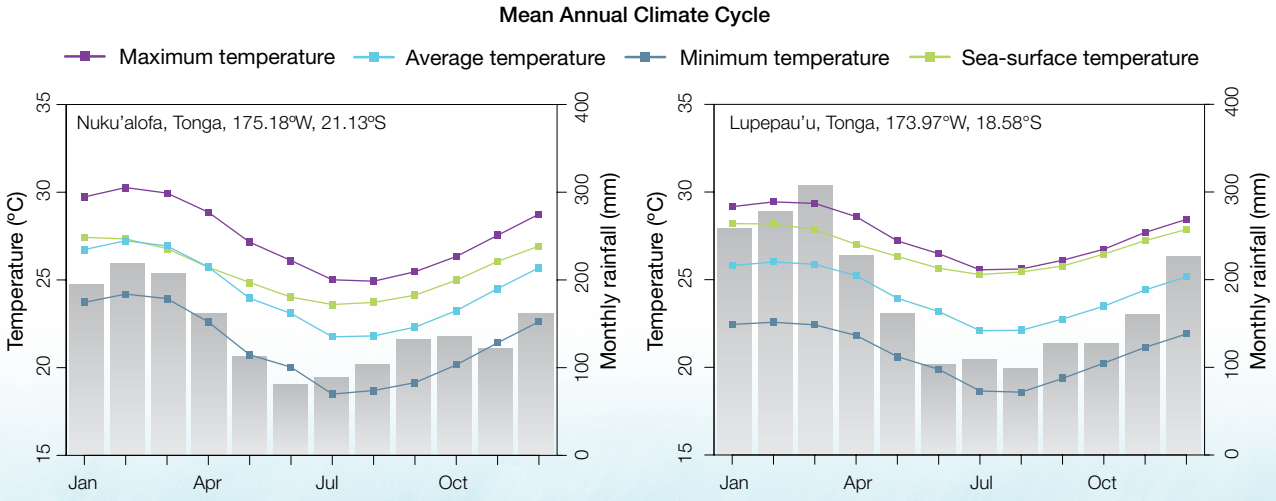

Figure 14.2: Mean annual cycle of rainfall (grey bars) and daily maximum, minimum and mean air temperatures at Nuku'alofa and (left) and Lupepau'u (right), and local sea-surface temperatures derived from the HadISST dataset (Volume 1, Table 2.3).

14.5 Climate Variability

Rainfall in Tonga has high variability from year-to-year. Both Nuku'alofa and Lupepau'u receive about three times as much rain in the wettest years as in the driest years. Much of this variability is driven by El Niño-Southern Oscillation (ENSO), as seen by the correlation coefficients in Table 14.2. In Nuku'alofa, El Niño events tend to bring cooler temperatures, especially in the dry season, most likely because of the cooler sea-surface temperatures around Tonga. El Niño years also tend to bring lower than normal rainfall during the wet season as the SPCZ usually moves away from Tonga to the north-east. In La Niña years the SPCZ moves closer and so wet season rainfall increases. Similar impacts are seen in Lupepau'u except temperatures in the wet season show no clear response to ENSO. Similar impacts are seen in ENSO Modoki events (Volume1, Section 3.4.1) to canonical El Niño and La Niña events but the influence is not as strong.

Some interdecadal variability in rainfall in the wet season can be linked with the Interdecadal Pacific Oscillation. The Southern Annular Mode influences air temperature to some extent in Tonga, and this is independent of the relationship between the Southern Annular Mode and ENSO.

Table 14.1: Correlation coefficients between indices of key large-scale patterns of climate variability and minimum and maximum temperatures (Tmin and Tmax) and rainfall at Nuku'alofa. Only correlation coefficients that are statistically significant at the 95% level are shown.

Climate feature/index		Dry season (May-October)			Wet season (November-April)		
		Tmin	Tmax	Rain	Tmin	Tmax	Rain
ENSO	Niño3.4	-0.72	-0.70		-0.37	-0.33	-0.61
	Southern Oscillation Index	0.66	0.73		0.38	0.35	0.69
Interdecadal Pacific Oscillation Index							-0.30
Southern Annular Mode Index			-0.30				
ENSO Modoki Index		-0.42	-0.36		-0.33	-0.26	-0.45
Number of years of data		58	60	65	58	60	66

Table 14.2: Correlation coefficients between indices of key large-scale patterns of climate variability and minimum and maximum temperatures (Tmin and Tmax) and rainfall at Lupepau'u. Only correlation coefficients that are statistically significant at the 95% level are shown.

Climate feature/Index		Dry Season (May–October)			Wet Season (November–April)		
		Tmin	Tmax	Rain	Tmin	Tmax	Rain
ENSO	Niño3.4	-0.53	-0.69				-0.58
	Southern Oscillation Index	0.40	0.67	0.26			0.66
Interdecadal Pacific Oscillation Index							
Southern Annular Mode Index						0.29	
ENSO Modoki Index					0.34		-0.39
Number of years of data		51	51	63	51	52	62

Taking observations, Tonga Meteorological Service

14.6 Observed Trends

14.6.1 Air Temperature

Trends for seasonal and annual mean air temperatures at Nuku'alofa (1950–2009) are positive (Figure 14.3), with the strongest trend (+0.16°C per decade) seen in wet season mean air temperatures. The trends in wet season maximum and minimum air temperatures are also considerably larger than that observed in the dry season (Table 14.3).

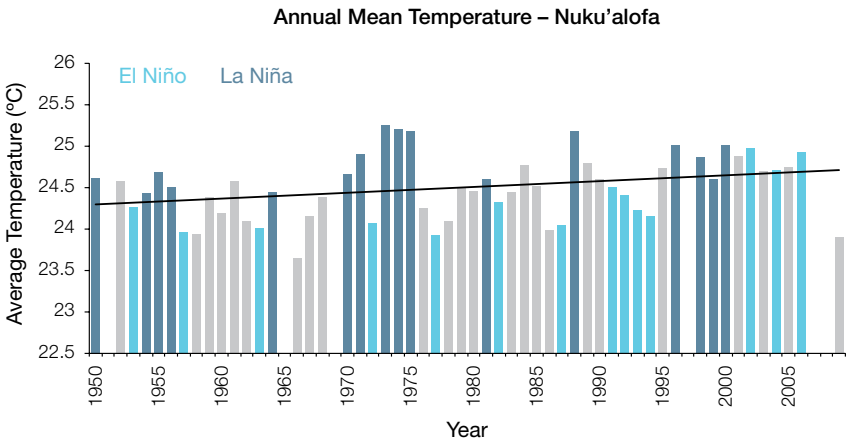

Figure 14.3: Annual mean air temperature at Nuku'alofa. Light blue, dark blue and grey bars denote El Niño, La Niña and neutral years respectively.

14.6.2 Rainfall

Annual and seasonal rainfall trends for Nuku'alofa and Lupepau'u for the period 1950–2009 are not statistically significant (Table 14.3; Figure 14.4).

14.6.3 Extreme Events

The tropical cyclone season in Tonga is between November and April. Occurrences outside this period are rare. The tropical cyclone archive for the Southern Hemisphere indicates that between the 1969/70 and 2009/10 seasons, the centre of 71 tropical cyclones passed within approximately 400 km of Nuku'alofa. This represents an average of 17 cyclones per decade. Tropical cyclones were most frequent in El Niño years (19 cyclones per decade) and least frequent in La Niña and ENSO-neutral years (16 cyclones per season). The interannual variability in the number of tropical cyclones in the vicinity of Nuku'alofa is large, ranging from zero in some seasons to five in the 2003/04 season (Figure 14.5). This high variability makes it difficult to identify any long-term trends in frequency.

Table 14.3: Annual and seasonal trends in maximum, minimum and mean air temperature (Tmax, Tmin and Tmean) and rainfall at Nuku'alofa and rainfall only at Lupepau'u for the period 1950–2009. Asterisks indicate significance at the 95% level. Persistence is taken into account in the assessment of significance as in Power and Kociuba (in press). The statistical significance of the air temperature trends is not assessed.

	Nuku'alofa Tmax (°C per 10 yrs)	Nuku'alofa Tmin (°C per 10 yrs)	Nuku'alofa Tmean (°C per 10 yrs)	Nuku'alofa Rain (mm per 10 yrs)	Lupepau'u Rain (mm per 10 yrs)
Annual	+0.10	+0.07	+0.07	-52	+7
Wet season	+0.14	+0.17	+0.16	-52	-7
Dry season	+0.06	+0.04	+0.05	+2	+20

14.6.4 Sea-Surface Temperature

Water temperatures around Tonga declined from the 1950s to the late 1980s (although there is some disagreement between datasets). This was followed by a period of warming (approximately 0.06°C per decade for 1970–present). Figure 14.8 shows the 1950–2000 sea-surface temperature changes (relative to a reference year of 1990) from three different large-scale sea-surface temperature datasets (HadSST2, ERSST and Kaplan Extended SST V2; Volume 1, Table 2.3). At these regional scales, natural variability may play a large role in the sea-surface temperature changes making it difficult to identify any long-term trends.

14.6.5 Ocean Acidification

Based the large-scale distribution of coral reefs across the Pacific and the seawater chemistry, Guinotte et al. (2003) suggested that seawater aragonite saturation states above 4 were optimal for coral growth and for the development of healthy reef ecosystems, with values from 3.5 to 4 adequate for coral growth, and values between 3 and 3.5, marginal. Coral reef ecosystems were not found at seawater aragonite saturation states below 3 and these conditions were classified as extremely marginal for supporting coral growth.

In the Tonga region, the aragonite saturation state has declined from about 4.5 in the late 18th century to an observed value of about 4.0 ± 0.1 by 2000.

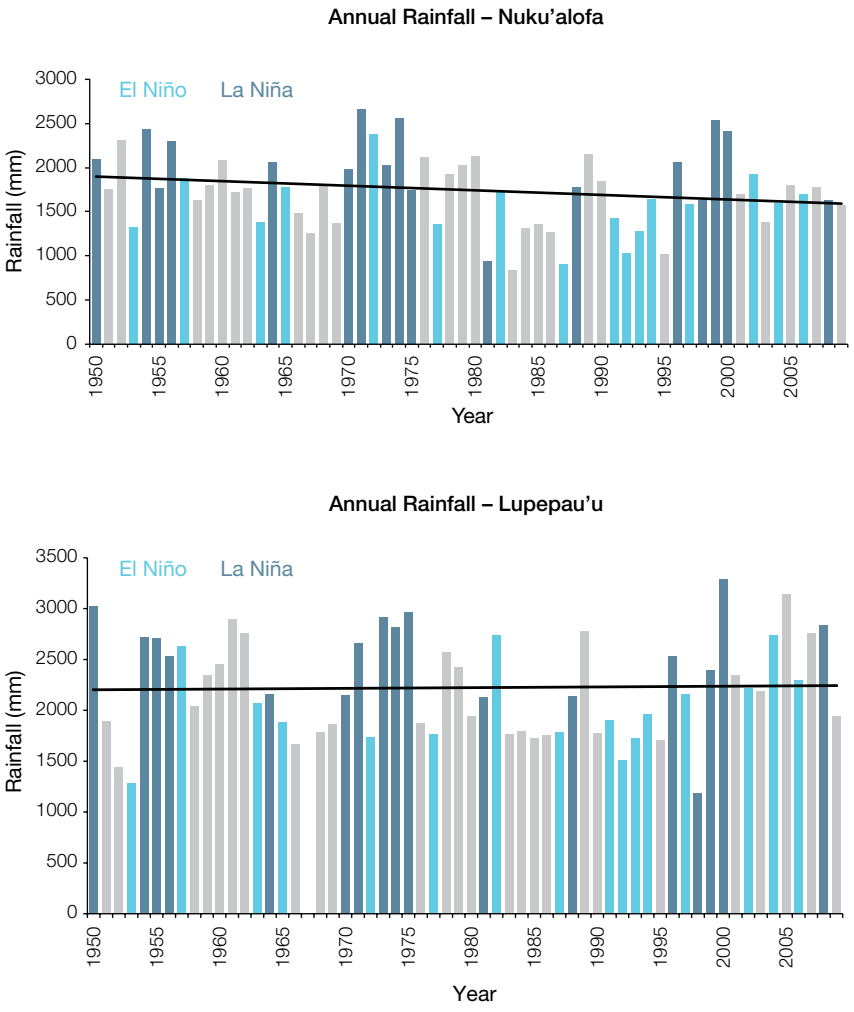

Figure 14.4: Annual rainfall at Nuku'alofa (top) and Lupepau'u (bottom). Light blue, dark blue and grey bars denote El Niño, La Niña and neutral years respectively.

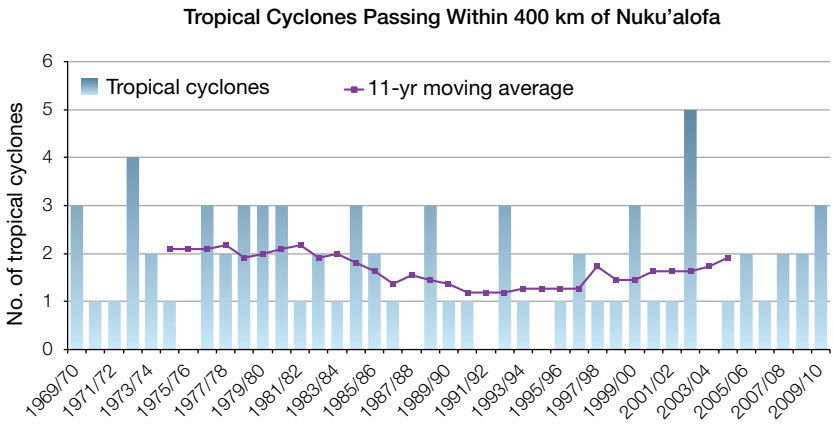

Figure 14.5: Tropical cyclones passing within 400 km of Nuku'alofa per season. The 11-year moving average is in purple.

14.6.6 Sea Level

Monthly averages of the historical tide gauge, satellite (since 1993) and gridded sea-level (since 1950) data agree well after 1993 and indicate interannual variability in sea levels of about 18 cm (estimated 5–95% range) after removal of the seasonal cycle (Figure 14.10). The sea-level rise near Tonga measured by satellite altimeters (Figure 14.6) since 1993 is over 6 mm per year, larger than the global average of 3.2 ± 0.4 mm per year. This rise is partly linked to a pattern related to climate variability from year to year and decade to decade (Figure 14.10).

14.6.7 Extreme Sea-Level Events

The annual climatology of the highest daily sea levels has been evaluated from hourly measurements by tide gauges at Nuku'alofa (Figure 14.7). High tides show relatively small variation throughout the year maximising in December and January. Average seasonal variations throughout the year are minimal. During La Niña years sea levels tend to be higher from May through August. During El Niño years the seasonal signal is negative from March through May and August through November, relative to the average signal, and close to the long-term average for the rest of the year. The top 10 sea-level events in the record occurred from December to March and at least half of these were associated with named tropical cyclones, indicating the importance of weather events in contributing to sea-level extremes.

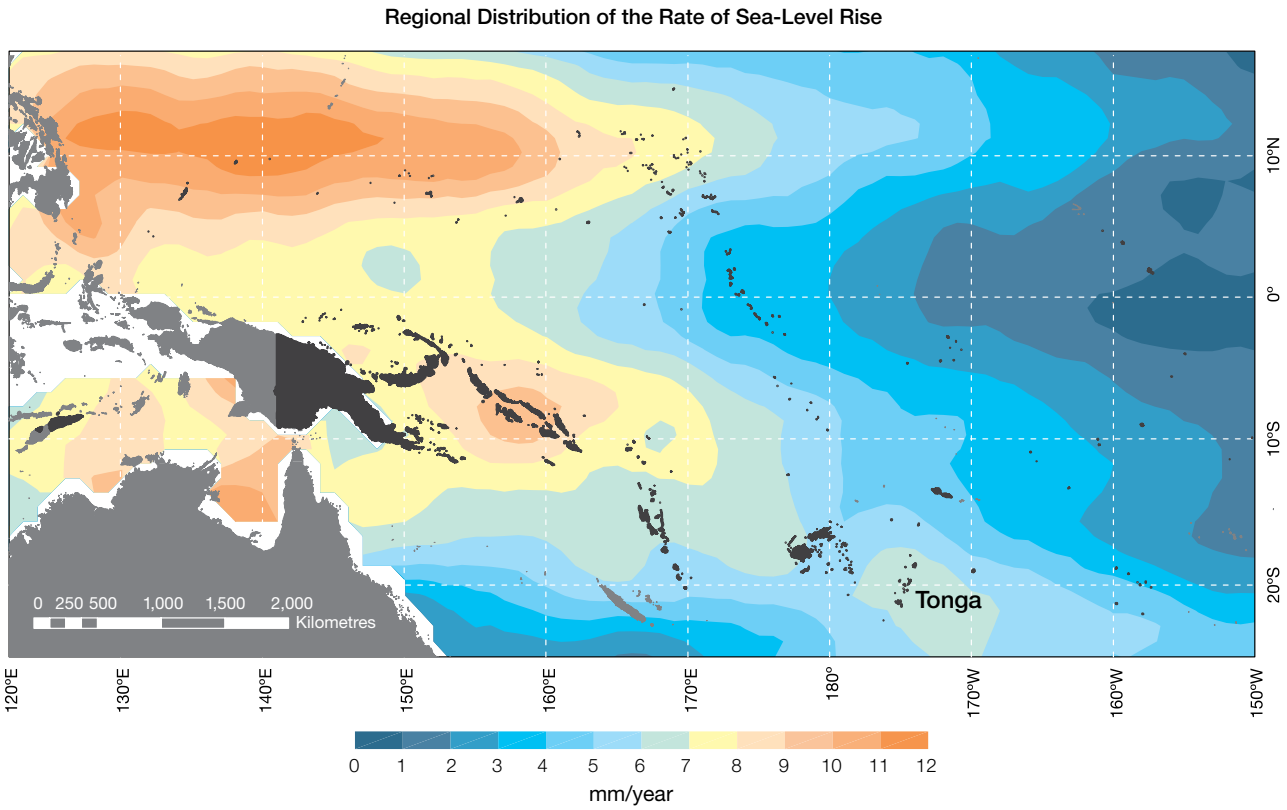

Figure 14.6: The regional distribution of the rate of sea-level rise measured by satellite altimeters from January 1993 to December 2010, with the location of Tonga indicated. Further detail about the regional distribution of sea-level rise is provided in Volume 1, Section 3.6.3.2.

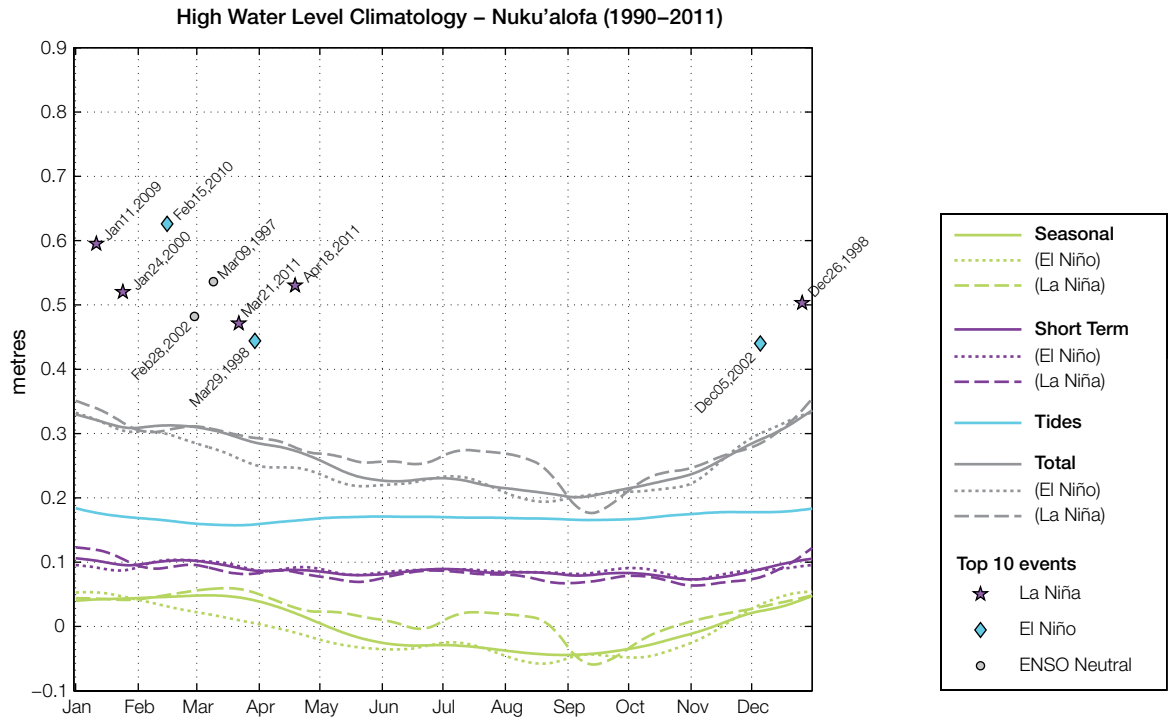

Figure 14.7: The annual cycle of high waters relative to Mean Higher High Water (MHHW) due to tides, short-term fluctuations (most likely associated with storms) and seasonal variations for Nuku'alofa. The tides and short-term fluctuations are respectively the 95% exceedence levels of the astronomical high tides relative to MHHW and short-term sea level anomaly fluctuations. Components computed only for El Niño and La Niña months are shown by dotted and dashed lines, and grey lines are the sum of the tide, short-term and seasonal components. The 10 highest sea-level events in the record relative to MHHW are shown and coded to indicate the phase of ENSO at the time of the extreme event.

14.7 Climate Projections

Climate projections have been derived from up to 18 global climate models from the CMIP3 database, for up to three emissions scenarios (B1 (low), A1B (medium) and A2 (high)) and three 20-year periods (centred on 2030, 2055 and 2090, relative to 1990). These models were selected based on their ability to reproduce important features of the current climate (Volume 1, Section 5.2.3), so projections from each of the models are plausible representations of the future climate. This means there is not one single projected future for Tonga, but rather a range of possible futures. The full range of these futures is discussed in the following sections.

These projections do not represent a value specific to any actual location, such as a town or city in Tonga. Instead, they refer to an average change over the broad geographic region encompassing the islands of Tonga and the surrounding ocean (Figure 1.1 shows the regional boundaries). Section 1.7 provides important information about interpreting climate model projections.

14.7.1 Temperature

Surface air temperature and sea-surface temperature are projected to continue to increase over the course of the 21st century. There is *very high* confidence in this direction of change because:

- Warming is physically consistent with rising greenhouse gas concentrations.
- All CMIP3 models agree on this direction of change.

Almost all of the CMIP3 models simulate a slight increase (<1°C) in annual and seasonal mean temperature by 2030, however by 2090 under the A2 (high) emissions scenario temperature increases of greater than 2.5°C are simulated by the majority of models (Table 14.4). Given the close relationship between surface air temperature and sea-surface temperature, a similar (or slightly weaker) rate of warming is projected for the surface ocean (Figure 14.8). There is *moderate* confidence in this range and distribution of possible futures because:

- There is generally a large discrepancy between modelled and observed temperature trends over the past 50 years in the vicinity of Tonga (Figure 14.8).

Interannual variability in surface air temperature and sea-surface temperature over Tonga is strongly influenced by ENSO in the current climate (Section 14.5). As there is no consistency in projections of future ENSO activity (Volume 1, Section 6.4.1) it is not possible to determine whether interannual variability in temperature will change in the future. However, ENSO is expected to continue to be an important source of variability for the region.

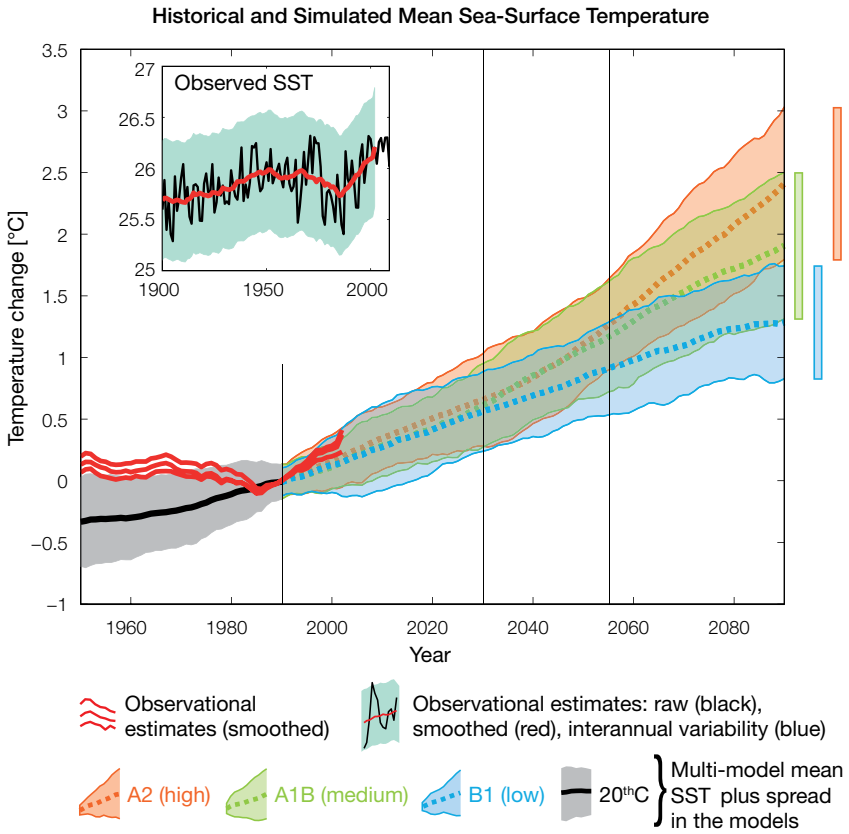

Figure 14.8: Historical climate (from 1950 onwards) and simulated historical and future climate for annual mean sea-surface temperature (SST) in the region surrounding Tonga, for the CMIP3 models. Shading represents approximately 95% of the range of model projections (twice the inter-model standard deviation), while the solid lines represent the smoothed (20-year running average) multi-model mean temperature. Projections are calculated relative to the 1980–1999 period (which is why there is a decline in the inter-model standard deviation around 1990). Observational estimates in the main figure (red lines) are derived from the HadSST2, ERSST and Kaplan Extended SST V2 datasets (Volume 1, Section 2.2.2). Annual average (black) and 20-year running average (red) HadSST2 data is also shown inset.

14.7.2 Rainfall

Wet Season (November-April)

Wet season rainfall is projected to increase over the course of the 21st century. There is *moderate* confidence in this direction of change because:

- An increase in wet season rainfall is consistent with the projected likely increase in the intensity of the South Pacific Convergence Zone (SPCZ), which lies over Tonga in this season (Volume 1, Section 6.4.5).
- The majority of CMIP3 models agree on this direction of change by 2090.

The majority of CMIP3 models simulate little change (-5% to 5%) in wet season rainfall by 2030, however by 2090 the majority simulate an increase (>5%), with a third simulating a large increase (>15%) under the A2 (high) emissions scenario (Table 14.4). There is *moderate* confidence in this range and distribution of possible futures because:

- In simulations of the current climate, the CMIP3 models generally locate the SPCZ in the correct location relative to Tonga in the wet season (Brown et al., 2011).
- The CMIP3 models are unable to resolve many of the physical processes involved in producing rainfall. As a consequence, they do not simulate rainfall as well as other variables such as temperature (Volume 1, Chapter 5).

Dry Season (May-October)

Dry season rainfall is projected to decrease over the course of the 21st century. There is *moderate* confidence in this direction of change because:

- Approximately half of the CMIP3 models agree on this direction of change by 2090.

The majority of CMIP3 models simulate little change (-5% to 5%) in dry season rainfall by 2030, however by 2090 under the higher emissions scenarios (i.e. A2 (high) and A1B (medium)) the models are approximately equally divided between a decrease (<-5%) and little change, with only a few models simulating an increase (>5%) (Table 14.4). There is *low* confidence in this range and distribution of possible futures because:

- In simulations of the current climate, some CMIP3 models have an SPCZ that extends too far east during the dry season, with too much rainfall over Tonga (Brown et al., 2011).
- The CMIP3 models are unable to resolve many of the physical processes involved in producing rainfall.

Annual

Little change is projected in total annual rainfall over the course of the 21st century. There is *low* confidence in this direction of change because:

- Only approximately half of the CMIP3 models agree on this direction of change by 2090.
- There is low confidence in the range and distribution of dry season rainfall projections, as discussed above.

Interannual variability in rainfall over Tonga is strongly influenced by ENSO in the current climate, via the movement of the SPCZ (Section 14.5). As there is no consistency in projections of future ENSO activity (Volume 1, Section 6.4.1) it is not possible to determine whether interannual variability in rainfall will change in the future.

14.7.3 Extremes

Temperature

The intensity and frequency of days of extreme heat are projected to increase over the course of the 21st century. There is *very high* confidence in this direction of change because:

- An increase in the intensity and frequency of days of extreme heat is physically consistent with rising greenhouse gas concentrations.
- All CMIP3 models agree on the direction of change for both intensity and frequency.

The majority of CMIP3 models simulate an increase of approximately 1°C in the temperature experienced on the 1-in-20-year hot day by 2055 under the B1 (low) emissions scenario, with an increase of over 2.5°C simulated by the majority of models by 2090 under the A2 (high) emissions scenario (Table 14.4). There is *low* confidence in this range and distribution of possible futures because:

- In simulations of the current climate, the CMIP3 models tend to underestimate the intensity and frequency of days of extreme heat (Volume 1, Section 5.2.4).
- Smaller increases in the frequency of days of extreme heat are projected by the CCAM 60 km simulations.

Rainfall

The intensity and frequency of days of extreme rainfall are projected to increase over the course of the 21st century. There is *high* confidence in this direction of change because:

- An increase in the frequency and intensity of extreme rainfall is consistent with larger-scale projections, based on the physical argument that the atmosphere is able to hold more water vapour in a warmer climate (Allen and Ingram, 2002; IPCC, 2007). It is also consistent with the projected likely increase in intensity of the SPCZ (Volume 1, Section 6.4.5).
- Almost all of the CMIP3 models agree on this direction of change for both intensity and frequency.

The majority of CMIP3 models simulate an increase of at least 15 mm in the amount of rain received on the 1-in-20-year wet day by 2055 under the B1 (low) emissions scenario, with an increase of at least 30 mm simulated by 2090 under the A2 (high) emissions scenario. The majority of models project that the current 1-in-20-year event will occur, on average, three to four times every year by 2055 under the B1 (low) emissions scenario and by five times every year by 2090 under the A2 (high) emissions scenario.

There is *low* confidence in this range and distribution of possible futures because:

- In simulations of the current climate, the CMIP3 models tend to underestimate the intensity and frequency of extreme rainfall (Volume 1, Section 5.2.4).
- The CMIP3 models are unable to resolve many of the physical processes involved in producing extreme rainfall.

Drought

Little change is projected in the incidence of drought over the course of the 21st century. There is *low* confidence in this direction of change because:

- There is only low confidence in the range of dry season rainfall projections (Section 14.7.2), which directly influences projections of future drought conditions.

Under the B1 (low) emissions scenario, the majority of CMIP3 models project that the frequency of mild drought will slightly increase from approximately seven to eight times every 20 years in 2030, to eight to nine times every 20 years by 2090. Under the A1B (medium) emissions scenario, the frequency of mild drought remains approximately constant from 2030 throughout the 21st century at seven to eight times every 20 years, while under the A2 (high) emissions scenario the frequency is projected to slightly decrease from eight to nine times every 20 years in 2030 to six to seven times by 2090. The majority of CMIP3 models project that moderate and severe droughts will occur approximately once to twice and once every 20 years respectively, across all time periods and emissions scenarios.

Tropical Cyclones

Tropical cyclone numbers are projected to decline in the south-east Pacific Ocean basin (0–40ºS, 170ºE–130ºW) over the course of the 21st century. There is *moderate* confidence in this direction of change because:

- Many studies suggest a decline in tropical cyclone frequency globally (Knutson et al., 2010).
- Tropical cyclone numbers decline in the south-east Pacific Ocean in the majority of assessment techniques.

Based on the direct detection methodologies (Curvature Vorticity Parameter (CVP) and the CSIRO Direct Detection Scheme (CDD) described in Volume 1, Section 4.8.2), 65% of projections show no change or a decrease in tropical cyclone formation when applied to the CMIP3 climate models for which suitable output is available. When these techniques are applied to CCAM, 100% of projections show a decrease in tropical cyclone formation. In addition, the Genesis Potential Index (GPI) empirical technique suggests that conditions for tropical cyclone formation will become less favourable in the south-east Pacific Ocean basin, for all analysed CMIP3 models. There is *moderate* confidence in this range and distribution of possible futures because in simulations of the current climate, the CVP, CDD and GPI methods capture the frequency of tropical cyclone activity reasonably well (Volume 1, Section 5.4).

Despite this projected reduction in total cyclone numbers, five of the six CCAM 60 km simulations show an increase in the proportion of the most severe cyclones. Most models also indicate a reduction in tropical cyclone wind hazard north of about 20ºS latitude and regions of increased hazard south of 20ºS latitude. This increase in wind hazard coincides with a poleward shift in the latitude at which tropical cyclones are most intense.

14.7.4 Ocean Acidification

The acidification of the ocean will continue to increase over the course of the 21st century. There is *very high* confidence in this projection as the rate of ocean acidification is driven primarily by the increasing oceanic uptake of carbon dioxide, in response to rising atmospheric carbon dioxide concentrations.

Projections from all analysed CMIP3 models indicate that the annual maximum aragonite saturation state will reach values below 3.5 by about 2035 and continue to decline thereafter (Figure 14.9; Table 14.4). There is *moderate* confidence in this range and distribution of possible futures because the projections are based on climate models without an explicit representation of the carbon cycle and with relatively low resolution and known regional biases.

The impact of acidification change on the health of reef ecosystems is likely to be compounded by other stressors including coral bleaching, storm damage and fishing pressure.

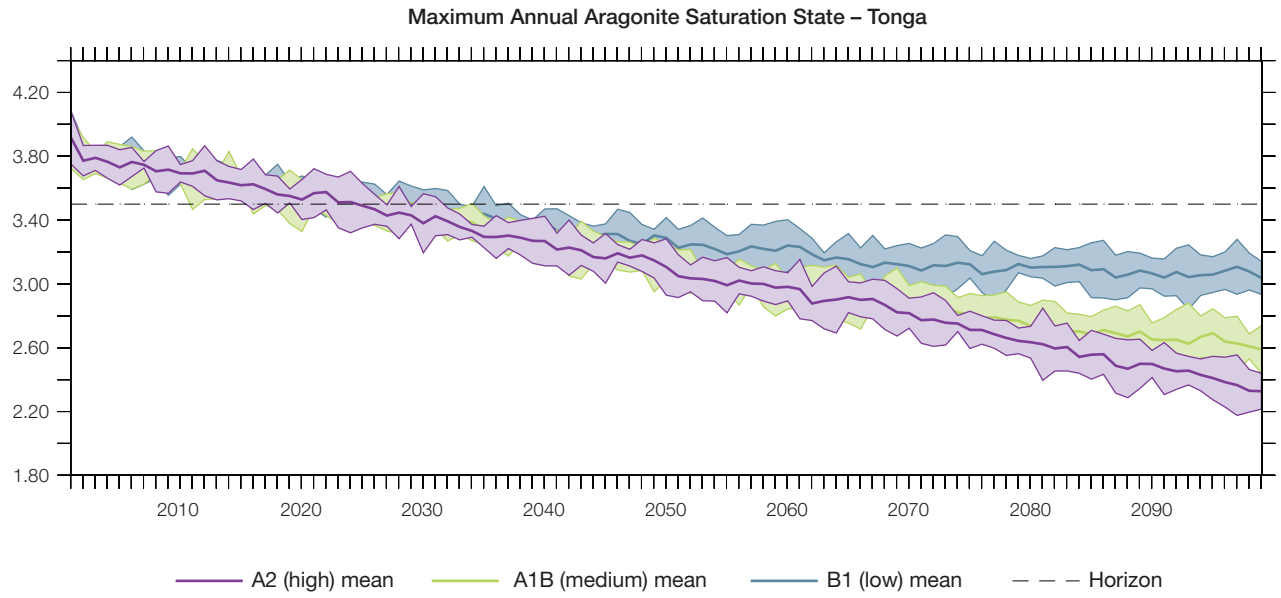

Figure 14.9: Multi-model projections, and their associated uncertainty (shaded area represents two standard deviations), of the maximum annual aragonite saturation state in the sea surface waters of the Tonga region under the different emissions scenarios. The dashed black line represents an aragonite saturation state of 3.5.

14.7.5 Sea Level

Mean sea level is projected to continue to rise over the course of the 21st century. There is *very high* confidence in this direction of change because:

- Sea-level rise is a physically consistent response to increasing ocean and atmospheric temperatures, due to thermal expansion of the water and the melting of glaciers and ice caps.
- Projections arising from all CMIP3 models agree on this direction of change.

The CMIP3 models simulate a rise of between approximately 5–15 cm by 2030, with increases of 20–60 cm indicated by 2090 under the higher-emissions scenarios (i.e. A2 (high), A1B (medium); Figure 14.10; Table 14.4).

There is *moderate* confidence in this range and distribution of possible futures because:

- There is significant uncertainty surrounding ice-sheet contributions to sea-level rise and a rise larger than projected above cannot be excluded (Meehl et al., 2007b). However, understanding of the processes is currently too limited to provide a best estimate or an upper bound (IPCC, 2007).
- Globally, since the early 1990s, sea level has been rising near the upper end of the above projections. During the 21st century, some studies (using semi-empirical models) project faster rates of sea-level rise.

Interannual variability of sea level will lead to periods of lower and higher regional sea levels. In the past, this interannual variability has been about 18 cm (5–95% range, after removal of the seasonal cycle; dashed lines in Figure 14.10 (a)) and it is likely that a similar range will continue through the 21st century. In addition, winds and waves associated with weather phenomena will continue to lead to extreme sea-level events.

In addition to the regional variations in sea level associated with ocean and mass changes, there are ongoing changes in relative sea level associated with changes in surface loading over the last glacial cycle (glacial isostatic adjustment) and local tectonic motions. The glacial isostatic motions are relatively small for the PCCSP region.

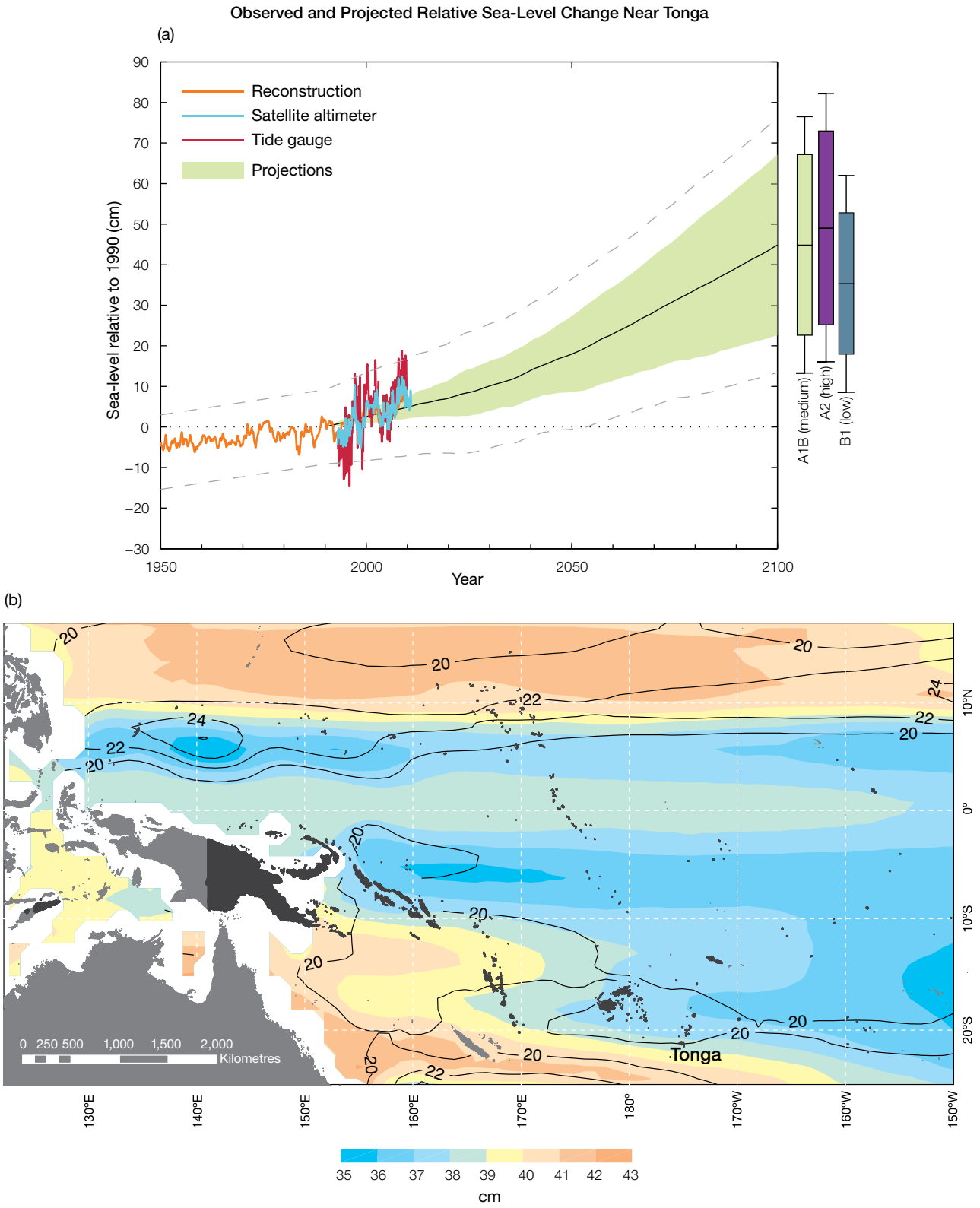

Figure 14.10: Observed and projected relative sea-level change near Tonga. (a) The observed in situ relative sea-level records are indicated in red, with the satellite record (since 1993) in light blue. The gridded sea level at Tonga (since 1950, from Church and White (in press)) is shown in orange. The projections for the A1B (medium) emissions scenario (5–95% uncertainty range) are shown by the green shaded region from 1990–2100. The range of projections for the B1 (low), A1B (medium) and A2 (high) emissions scenarios are also shown by the bars on the right. The dashed lines are an estimate of interannual variability in sea level (5–95% range about the long-term trends) and indicate that individual monthly averages of sea level can be above or below longer-term averages. (b) The projections (in cm) for the A1B (medium) emissions scenario in the Tonga region for the average over 2081–2100 relative to 1981–2000 are indicated by the shading, with the estimated uncertainty in the projections indicated by the contours (in cm).

14.7.6 Projections Summary

The projections presented in Section 14.7 are summarised in Table 14.4. For detailed information regarding the various uncertainties associated with the table values, refer to the preceding text in Sections 14.7 and 1.7, in addition to Chapters 5 and 6 in Volume 1. When interpreting the differences between projections for the A2 (high), A1B (medium), and B1 (low) emissions scenarios, it is also important to consider the emissions pathways associated with each scenario (Volume 1, Figure 4.1) and the fact that a slightly different subset of models was available for each (Volume 1, Appendix 1).

Table 14.4: Projected change in the annual and seasonal-mean climate for Tonga, under the B1 (low; blue), A1B (medium; green) and A2 (high; purple) emissions scenarios. Projections are given for three 20-year periods centred on 2030 (2020–2039), 2055 (2046–2065) and 2090 (2080–2099), relative to 1990 (1980–1999). Values represent the multi-model mean change ± twice the inter-model standard deviation (representing approximately 95% of the range of model projections), except for sea level where the estimated mean change and the 5–95% range are given (as they are derived directly from the Intergovernmental Panel on Climate Change Fourth Assessment Report values). The confidence (Section 1.7.2) associated with the range and distribution of the projections is also given (indicated by the standard deviation and multi-model mean, respectively). See Volume 1, Appendix 1 for a complete listing of CMIP3 models used to derive these projections.

Variable	Season	2030	2055	2090	Confidence
Surface air temperature (°C)	Annual	+0.6 ± 0.4 +0.7 ± 0.5 +0.7 ± 0.4	+1.0 ± 0.5 +1.3 ± 0.6 +1.4 ± 0.4	+1.4 ± 0.6 +2.1 ± 0.8 +2.6 ± 0.7	Moderate
Maximum temperature (°C)	1-in-20-year event	N/A	+1.0 ± 0.7 +1.4 ± 0.7 +1.4 ± 0.6	+1.3 ± 0.6 +2.1 ± 0.9 +2.4 ± 1.4	Low
Minimum temperature (°C)	1-in-20-year event	N/A	+1.1 ± 1.7 +1.5 ± 1.4 +1.4 ± 1.7	+1.5 ± 1.6 +2.0 ± 2.1 +2.3 ± 1.7	Low
Total rainfall (%)*	Annual	+2 ± 13 +1 ± 13 +3 ± 13	+1 ± 10 +3 ± 14 +5 ± 12	+3 ± 14 +3 ± 14 +9 ± 18	Low
Wet season rainfall (%)*	November-April	+4 ± 12 +2 ± 14 +5 ± 15	+4 ± 14 +6 ± 18 +9 ± 15	+6 ± 20 +8 ± 18 +16 ± 19	Moderate
Dry season rainfall (%)*	May-October	0 ± 18 -2 ± 19 +1 ± 13	-3 ± 15 0 ± 21 +1 ± 16	-1 ± 18 -3 ± 20 -1 ± 26	Low
Sea-surface temperature (°C)	Annual	+0.6 ± 0.3 +0.6 ± 0.3 +0.7 ± 0.4	+0.9 ± 0.4 +1.2 ± 0.4 +1.3 ± 0.4	+1.3 ± 0.5 +1.9 ± 0.6 +2.4 ± 0.6	Moderate
Aragonite saturation state (Ωar)	Annual maximum	+3.4 ± 0.1 +3.4 ± 0.1 +3.4 ± 0.1	+3.2 ± 0.1 +3.0 ± 0.1 +3.0 ± 0.1	+3.0 ± 0.1 +2.6 ± 0.1 +2.4 ± 0.1	Moderate
Mean sea level (cm)	Annual	+10 (5–16) +10 (4–16) +10 (3–17)	+19 (10–27) +21 (10–31) +20 (9–31)	+32 (16–47) +39 (20–59) +41 (21–62)	Moderate

*The MIROC3.2(medres) and MIROC3.2(hires) models were eliminated in calculating the rainfall projections, due to their inability to accurately simulate present-day activity of the South Pacific Convergence Zone (Volume 1, Section 5.5.1).